scientific reports

Check for updates

OPEN

Preserved white matter integrity is a promising indicator of cognitive resilience in Parkinson's disease

Zhichun Chen[1,2,6], Weiting Tang[1,6], Yuxuan Shi[1], Sheng Hu[1], Bin Chen[1], Jindong Ding Petersen[1,3], Binwen Huang[4], Jun Liu[2]✉ & Yong You[1,5]✉

Cognitive and motor impairment in Parkinson's disease (PD) is linked to white matter integrity, yet the prognostic utility of white matter-derived imaging metrics for predicting cognitive and motor decline remains underexplored. Leveraging longitudinal clinical and neuroimaging data from the Parkinson's Progression Markers Initiative (PPMI) cohort, this study identified microstructural integrity of several specific white matter tracts, including corpus callosum (body, genu, and splenium) and right inferior cerebellar peduncle, as potential indicators for longitudinal cognitive decline in PD patients. Specifically, over a mean follow-up period of 49.13 months, reduced integrity in these tracts was linked to accelerated cognitive decline, while preserved integrity was associated with slower cognitive decline. In contrast, no white matter-based imaging metrics demonstrated significant associations with motor decline after corrections for multiple testing. These findings underscore the critical role of white matter integrity as a potential indicator for tracking longitudinal cognitive deterioration in PD. By pinpointing specific white matter alterations linked to cognitive progression, this study offers valuable insights into the neural substrates of cognitive deficits in PD. Future research should focus on elucidating the molecular mechanisms underlying the relationship between white matter integrity and cognitive function, potentially informing targeted therapeutic strategies to mitigate cognitive impairment and enhance quality of life for PD patients.

Keywords Parkinson's disease, White matter integrity, Cognitive function, Motor decline, Cognitive resilience

Parkinson's disease (PD), a progressive neurodegenerative disorder, poses substantial challenges to individuals and healthcare systems globally. With a prevalence of approximately 1% in individuals over 60 years old and rising incidence rates in aging populations, PD is a major contributor to the global burden of neurological diseases[1,2]. The hallmark motor symptoms of PD, including bradykinesia, rigidity, and tremors, are often accompanied by a spectrum of non-motor manifestations that complicate disease management and substantially exacerbate the overall disease burden. Among these, cognitive decline stands out as one of the most critical non-motor features, occurring nearly six times more frequently in PD patients than in healthy individuals[3]. Cognitive decline can manifest at any disease stage, including the prodromal phase and early stages of the disorder[4,5], and is associated with accelerated disease progression and poorer prognosis[3,6]. The urgent need for early diagnosis and intervention strategies to mitigate both cognitive and motor impairments in PD is highlighted by their profound impact on the patient quality of life and healthcare costs. Understanding and predicting the longitudinal trajectories of both motor and cognitive decline in PD is crucial for developing targeted interventions to alleviate the medical burden associated with this debilitating disease.

Recently, Owens-Walton et al.. (2024) have reported widespread microstructural alterations in white matter tracts across all stages of PD, which are associated with cognitive impairment[7]. Our previous work demonstrated that PD patients exhibit age-dependent impairment in multiple white matter tracts, significantly correlating with

[1]Department of Neurology, The Second Affiliated Hospital of Hainan Medical University, Haikou 570311, China. [2] Department of Neurology and Institute of Neurology, Ruijin Hospital affiliated to Shanghai Jiao Tong University School of Medicine, Shanghai 200025, China. [3]School of Public Health, Key Laboratory of Tropical Translational Medicine of Ministry of Education, Hainan Medical University, Haikou 571199, China. [4]School of Intelligent Medicine and Technology (Big Data Research Center), Key Laboratory of Tropical Translational Medicine of Ministry of Education, Hainan Medical University, Haikou 571199, China. [5]International Center for Aging and Cancer (ICAC), Hainan Medical University, Haikou 571199, China. [6]Zhichun Chen and Weiting Tang contributed equally to this work. ✉email: jly0520@hotmail.com; hy213440@muhn.edu.cn

cognitive impairment[8]. This deterioration in white matter integrity leads to substantial changes in the topology of structural networks in PD, further contributing to age-dependent cognitive decline[8]. Additionally, small-world properties within the structural network have been significantly linked to declines in verbal memory among PD patients[9]. These findings suggest that disruptions in white matter integrity play a critical role in the progression of cognitive decline in PD. In contrast, the relationship between white matter integrity and motor impairment is more complex and controversial. While a previous study showed that impaired white matter integrity is not associated with the severity of motor symptoms[10], a large-scale study encompassing 17 cohorts worldwide reported a significant association between loss of white matter integrity and clinical motor decline[7]. White matter hyperintensities represent areas of abnormal white matter tissue that can be associated with various pathological processes, including demyelination, gliosis, and ischemia. Interestingly, white matter hyperintensities have garnered attention as potential predictive biomarkers for cognitive impairment but not for motor decline in PD patients[11,12]. Consistently, a recent longitudinal study also found that baseline volume of white matter hyperintensities has no predictive value for motor decline in PD patients[13]. However, a systematic review and meta-analysis of cross-sectional studies indicated that PD patients with higher levels of white matter hyperintensities exhibit worse motor symptoms compared to those with lower white matter hyperintensities burden[14]. Therefore, while the disruption of white matter integrity is clearly associated with cognitive decline, the relationship between white matter integrity and motor deterioration remains a subject of ongoing debate.

White matter lesions in PD are characterized by impaired myelination or axon integrity in central nervous system[15,16]. These pathological changes are significantly associated with PD-related cognitive impairment[7,16]. Therefore, we hypothesized that higher white matter integrity, measured by diffusion tensor imaging (DTI), may be an indicator of cognitive resilience in PD patients. To validate this hypothesis, we evaluated the associations between white matter-based metrics and cognitive performance using complementary analytical approaches: cross-sectional analysis to establish baseline relationships at study entry, and longitudinal analysis to assess the long-term relationships over time within the Parkinson's Progression Markers Initiative (PPMI) cohort. Specifically, logistic regression analysis was employed to evaluate the associations between white matter metrics and baseline cognitive states cross-sectionally. Longitudinally, logistic regression was also conducted to examine the associations between white matter metrics and risk of future cognitive decline in PD patients. Moreover, to address inconsistent findings regarding the association between white matter lesions and motor dysfunction in PD, we also assessed the associations between white matter metrics and future motor decline. Furthermore, we evaluated the effects of white matter integrity on longitudinal cognitive decline using linear mixed-effects analyses to further validate several major findings. These methodological approaches aimed to comprehensively characterize the potential associations between white matter-based metrics and longitudinal cognitive and motor decline in PD.

Results

The comparisons of clinical characteristics

At baseline, PD patients demonstrated significantly more severe motor and cognitive impairments relative to healthy control participants, as reflected in key clinical assessments summarized in Table 1. Specifically, PD patients presented with significantly higher scores on the Movement Disorder Society Unified Parkinson's Disease Rating Scale part III (UPDRS-III), indicating greater motor impairment, as well as elevated total UPDRS scores. Cognitively, the PD group showed markedly lower performance on both the Symbol Digit Modalities Test (SDMT) and the Montreal Cognitive Assessment (MoCA), suggesting deficits in processing speed and overall cognitive function. Importantly, other baseline demographic and clinical characteristics, including age, sex distribution, and years of education, did not differ significantly between the two groups, supporting

Groups/Statistics Clinical variables	Control at baseline ($n=121$)	PD at baseline ($n=121$)	PD after Follow-up ($n=121$)	*P*-value (Control vs. PD at baseline)	*P*-value (Baseline vs. Follow-up in PD)
Age, years	59.69 ± 10.76	60.46 ± 9.15	64.31 ± 9.25	$P>0.05$	$P<0.0001$
Sex (Male/Female)	78/43	79/42	79/42	$P>0.05$	-
Education, years	16.07 ± 2.59	15.57 ± 2.77	15.57 ± 2.77	$P>0.05$	-
Disease duration, years	-	1.42 ± 1.46	5.52 ± 1.72	-	$P<0.0001$
UPDRS-III	0.97 ± 1.86	20.11 ± 9.89	21.87 ± 12.67	$P<0.0001$	$P>0.05$
Total UPDRS	1.88 ± 2.55	32.57 ± 14.65	40.15 ± 18.85	$P<0.0001$	$P<0.0001$
LNS	11.33 ± 2.32	10.80 ± 2.73	10.25 ± 2.99	$P>0.05$	$P<0.01$
SFT	47.00 ± 14.64	50.31 ± 11.46	51.10 ± 12.62	$P>0.05$	$P>0.05$
SDMT	48.94 ± 11.12	41.71 ± 10.78	40.48 ± 13.01	$P<0.0001$	$P>0.05$
MoCA	28.16 ± 1.33	27.13 ± 2.46	27.29 ± 2.88	$P<0.0001$	$P>0.05$

Table 1. The clinical assessments at baseline and after follow-up. The data were shown as the mean ± SD. Unpaired Student's t-test or χ^2 test (for categorical variable) was used to compare clinical variables between control and PD at baseline. Paired Student's t-test was utilized to compare clinical variables at baseline and follow-up in PD patients. $P<0.05$ was considered statistically significant. Abbreviations: PD, Parkinson's disease; MoCA, Montreal Cognitive Assessment; LNS, Letter Number Sequencing Test; SDMT, Symbol Digit Modalities Test; SFT, Semantic Fluency Test; UPDRS-III, Unified Parkinson's Disease Rating Scale part III; UPDRS, Unified Parkinson's Disease Rating Scale.

the comparability of the cohorts aside from disease-specific impairments. In 121 patients with longitudinal clinical and DTI data in PPMI database, we assessed whether cognitive and motor function were changed after 1 ~ 5 year of follow-up. The average follow-up duration was 49.31 ± 10.36 months (mean ± standard deviation [SD]). As presented in Table 1; Fig. 1, while Letter Number Sequencing Test (LNS) scores significantly declined over the follow-up period ($P < 0.01$), the scores for Semantic Fluency Test (SFT), SDMT, and MoCA did not exhibit significant changes, indicating most cognitive domains in PD patients remain stable over the follow-up duration. Regarding motor assessments, our analysis revealed no significant differences in UPDRS-III scores from baseline to follow-up; however, total UPDRS scores showed a significant increase at follow-up ($P < 0.0001$). Despite group-level stability in the scores of clinical assessments, individual trajectories revealed considerable heterogeneity. A substantial proportion of patients showed longitudinal changes in cognitive and motor scores. Specifically, the reductions of cognitive scores were observed in 44.6% (54/121) of the patients on the SFT, 49.6% (60/121) on the SDMT, and 31.4% (38/121) on the MoCA. In contrast, 54.5% (60/110) of the patients exhibited an increase in UPDRS-III scores, reflecting concurrent motor progression. This divergence, where group-level stability masked individual deterioration, underscored the need for person-specific risk prediction models.

The associations between white matter-based metrics and baseline cognitive decline

To investigate the relationships between white matter microstructural integrity and baseline cognitive decline in patients with PD, we performed logistic regression analyses examining fractional anisotropy (FA) and mean diffusivity (MD) across 34 major white matter tracts derived from the Johns Hopkins University ICBM-DTI atlas. These tracts were selected based on their established roles in supporting human cognitive and motor functions, as evidenced by prior neuroanatomical and clinical studies[15–18]. The analytical approach operationalized baseline cognitive decline in PD patients by applying a normative threshold: individuals were classified as having significant cognitive impairment if they scored >2 SD below the mean of healthy controls on one of the cognitive tests, enabling dichotomous classification for subsequent regression modeling of white matter associations. This method is particularly valuable for neuropsychological tests lacking established normative cutoffs, such

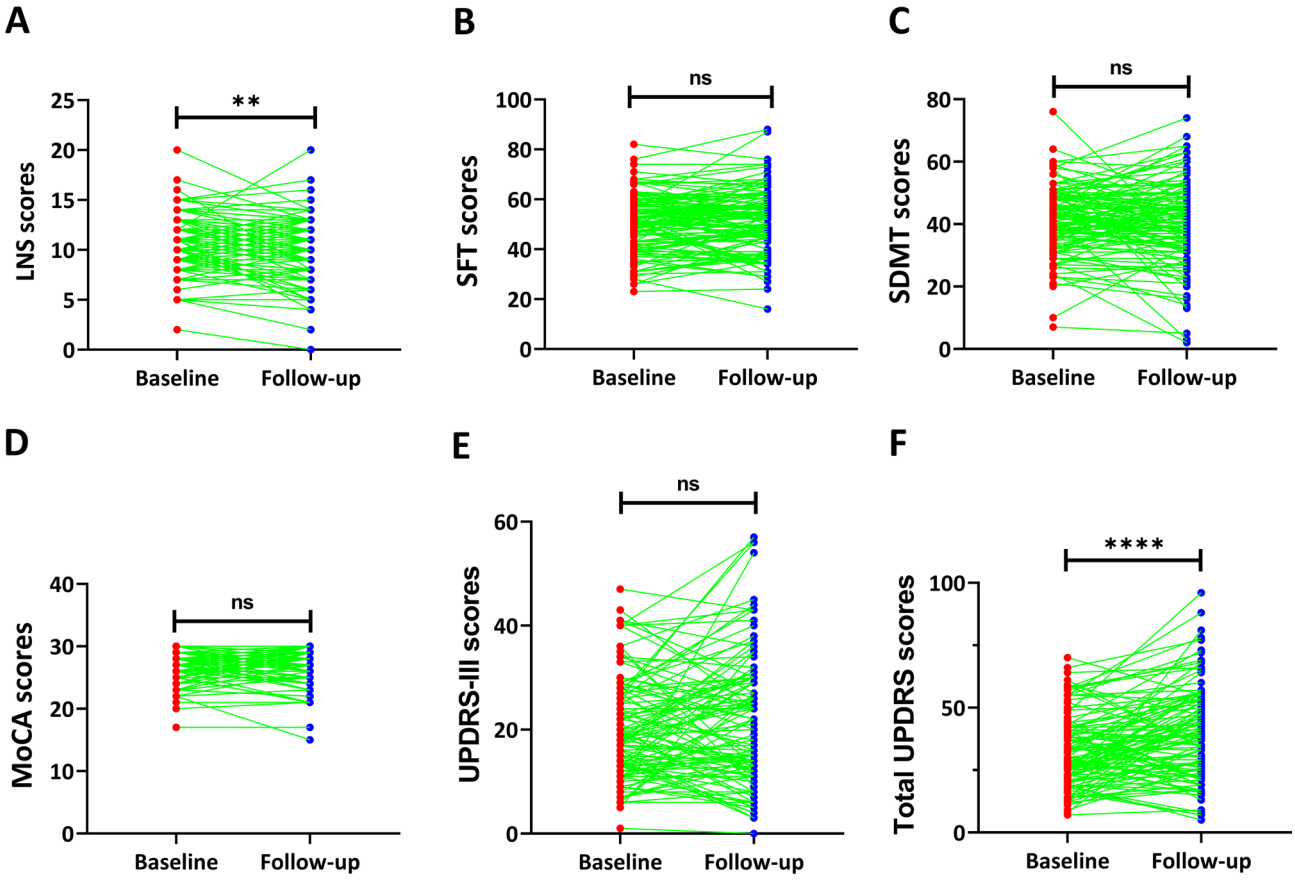

Fig. 1. Longitudinal changes of cognitive and motor symptoms in PD patients. (**A**-**F**) Group differences in the scores of LNS, SFT, SDMT, MoCA, UPDRS-III, and total UPDRS between baseline and follow-up. Paired Student's t-test (Baseline vs. Follow-up) were utilized to compare above clinical variables. $P < 0.05$ was considered statistically significant. $^{**}P < 0.01$, $^{****}P < 0.0001$. Abbreviations: LNS, Letter Number Sequencing Test; MoCA, Montreal Cognitive Assessment; SDMT, Symbol Digit Modalities Test; SFT, Semantic Fluency Test; UPDRS, Unified Parkinson's Disease Rating Scale; UPDRS-III, Unified Parkinson' s Disease Rating Scale Part III.

as LNS, SDMT, and SFT. All logistic regression models incorporated covariate adjustment for age, sex, years of education, and disease duration, with false discovery rate (FDR) correction applied for the 34 tracts for each cognitive scale. We found no tract-specific FA values showed a significant association with baseline decline in the LNS test scores (Table S1). Regarding the SFT, no PD patients met the criterion for baseline cognitive decline (scoring >2 SD below the mean of SFT in healthy control); therefore, statistical analysis was not applicable for logistic regression. In contrast, higher FA values in several white matter tracts, including genu (OR = 0.36 [0.15, 0.79], P = 0.0147, FDR-corrected P >0.05), body (OR = 0.38 [0.15, 0.88], P = 0.0291, FDR-corrected P >0.05), splenium (OR = 0.39 [0.17, 0.84], P = 0.0208, FDR-corrected P >0.05) of CC and bilateral inferior cerebellar peduncle (ICP; Right: OR = 0.28 [0.09, 0.67], P = 0.0138, FDR-corrected P >0.05; Left: OR = 0.39 [0.15, 0.81], P = 0.0276, FDR-corrected P >0.05), were associated with a lower likelihood of baseline SDMT scores decline (Table S2), though none survived FDR correction. Moreover, higher FA values in splenium of CC (OR = 0.61 [0.36, 0.98], P = 0.0473, FDR-corrected P >0.05) and right cerebral peduncle (OR = 0.60 [0.35, 0.98], P = 0.0488, FDR-corrected P >0.05) were linked to a lower probability of baseline decline on MoCA scores (Table S3) and none survived FDR correction.

At an uncorrected threshold of P < 0.05, several tract-specific MD values showed associations with baseline cognitive decline in PD patients, as summarized in Tables S4–S6. Specifically, higher MD values in bilateral corticospinal tract (Right: OR = 2.37 [1.04, 6.02], P = 0.0479, FDR-corrected P > 0.05; Left: OR = 2.46 [1.12, 5.99], P = 0.0305, FDR-corrected P > 0.05) were associated with an increased likelihood of baseline LNS score decline (Table S4), though these associations did not survive FDR correction. Elevated MD values in several white matter tracts, including genu (OR = 2.45 [1.18, 5.49], P = 0.0194, FDR-corrected P > 0.05), body (OR = 2.34 [1.04, 5.69], P = 0.0445, FDR-corrected P > 0.05), splenium (OR = 2.11 [1.04, 4.52], P = 0.0418, FDR-corrected P > 0.05) of CC, were associated with an increased likelihood of baseline SDMT score decline (Table S5), but again, none remained significant after FDR correction. In contrast, no tract-specific MD values were significantly associated with baseline decline in MoCA scores, even at the uncorrected level (Table S6).

We additionally conducted logistic regression analyses for seven topological metrics of the white matter network, including global efficiency (GE), local efficiency (LE), and small-worldness metrics (clustering coefficient [Cp], characteristic path length [Lp], normalized clustering coefficient [γ], normalized characteristic path length [λ], and small-worldness [σ]); however, none survived FDR correction (Table S7).

The associations between white matter-based metrics and longitudinal cognitive decline

Building on these findings, we evaluated the associations between white matter integrity metrics and longitudinal cognitive decline using logistic regression. Unlike cross-sectional analyses, these models were adjusted for age, sex, educational attainment, follow-up duration, baseline cognitive function, and disease duration. Cognitive decline at follow-up was operationally defined as cognitive test score falling > 2 SD below mean scores of one or more cognitive tests of PD patients at baseline. This approach reliably identified individuals exhibiting cognitive impairment during follow-up. For SDMT, we found higher FA values in several white matter tracts, including genu (OR = 0.23 [0.07, 0.59], P = 0.0042, FDR-corrected P = 0.0341), body (OR = 0.12 [0.02, 0.42], P = 0.0034, FDR-corrected P = 0.0341), splenium (OR = 0.22 [0.07, 0.55], P = 0.0030, FDR-corrected P = 0.0341) of CC and right ICP (OR = 0.08 [0.01, 0.42], P = 0.0139, FDR-corrected P = 0.0471), were associated with a lower likelihood of SDMT score decline at follow-up (Table 2). At the uncorrected threshold of P < 0.05, we similarly found higher FA values in several white matter tracts were associated with a lower probability of decline in LNS scores at follow-up (Table S8). However, these associations did not survive FDR correction (Table S8). In contrast, no tract-specific FA values demonstrated a significant association with longitudinal MoCA scores decline (Table S9).

The associations between tract-specific MD values and longitudinal cognitive decline in PD patients were shown in Table 3 and Table S10-11. After FDR correction, higher MD values in several white matter tracts, including genu (OR = 3.08 [1.34, 7.70], P = 0.0089, FDR-corrected P < 0.05), body (OR = 5.88 [2.06, 23.44], P = 0.0029, FDR-corrected P < 0.05), and splenium (OR = 5.20 [2.04, 18.23], P = 0.0022, FDR-corrected P < 0.05) of CC, were associated with an increased likelihood of longitudinal SDMT scores decline (Table 3). At an uncorrected threshold of P < 0.05, elevated MD values in several white matter tracts, including genu (OR = 2.97 [1.31, 7.25], P = 0.0100, FDR-corrected P > 0.05), body (OR = 3.59 [1.38, 11.20], P = 0.0135, FDR-corrected P > 0.05), and splenium (OR = 3.40 [1.45, 9.40], P = 0.0083, FDR-corrected P > 0.05) of CC, were associated with a higher likelihood of longitudinal LNS scores decline (Table S10). No tract-specific MD values demonstrated a significant association with longitudinal MoCA score decline (Table S11).

In the longitudinal analysis, we also performed logistic regression analyses for seven topological metrics of the white matter network, whereas none survived FDR correction (Table S12).

The associations between white matter-based metrics and longitudinal motor decline

As shown in Tables S13–S14, no significant associations were observed between tract-specific FA or MD values and longitudinal increases in UPDRS-III scores after FDR correction. However, higher FA values in right anterior corona radiata (OR = 0.34 [0.16, 0.66], P = 0.0025, FDR-corrected P < 0.05), right superior longitudinal fasciculus (OR = 0.36 [0.17, 0.69], P = 0.0037, FDR-corrected P < 0.05), left superior longitudinal fasciculus (OR = 0.39 [0.19, 0.72], P = 0.0042, FDR-corrected P < 0.05), and right inferior fronto-occipital fasciculus (OR = 0.31 [0.13, 0.67], P = 0.0055, FDR-corrected P < 0.05) were associated with a lower likelihood of longitudinal increase in total UPDRS scores (Table S15). In addition, at an uncorrected threshold of P < 0.05, higher MD values in several white matter tracts, such as right superior corona radiata (OR = 2.07 [1.11, 4.16], P = 0.0288, FDR-corrected P > 0.05) and left superior corona radiata (OR = 2.28 [1.18, 5.01], P = 0.0244, FDR-corrected P > 0.05), were linked to a higher risk of total UPDRS score increase (Table S16), though these associations did not survive FDR correction.

Tracts Statistics	OR	Lower_CI	Upper_CI	*P*-value	FDR-corrected *P*-value
Genu of corpus callosum	**0.23**	**0.07**	**0.59**	**0.0042**	**0.0341**
Body of corpus callosum	**0.12**	**0.02**	**0.42**	**0.0034**	**0.0341**
Splenium of corpus callosum	**0.22**	**0.07**	**0.55**	**0.0030**	**0.0341**
Fornix	0.34	0.10	0.92	0.0580	0.1096
Right corticospinal tract	0.87	0.34	2.18	0.7608	0.8335
Left corticospinal tract	1.03	0.43	2.46	0.9521	0.9808
Right inferior cerebellar peduncle	**0.08**	**0.01**	**0.42**	**0.0139**	**0.0471**
Left inferior cerebellar peduncle	0.25	0.05	0.69	0.0308	0.0782
Right superior cerebellar peduncle	0.43	0.17	0.99	0.0564	0.1096
Left superior cerebellar peduncle	0.36	0.12	0.91	0.0424	0.0902
Right cerebral peduncle	**0.18**	**0.04**	**0.54**	**0.0060**	**0.0341**
Left cerebral peduncle	**0.26**	**0.08**	**0.68**	**0.0106**	**0.0449**
Right anterior limb of internal capsule	**0.29**	**0.10**	**0.69**	**0.0086**	**0.0419**
Left anterior limb of internal capsule	**0.27**	**0.09**	**0.65**	**0.0060**	**0.0341**
Right posterior limb of internal capsule	0.50	0.19	1.25	0.1488	0.2200
Left posterior limb of internal capsule	0.99	0.40	2.41	0.9808	0.9808
Right retrolenticular part of internal capsule	0.57	0.19	1.42	0.2588	0.3520
Left retrolenticular part of internal capsule	0.48	0.18	1.14	0.1122	0.1733
Right anterior corona radiata	0.28	0.08	0.76	0.0213	0.0653
Left anterior corona radiata	**0.20**	**0.06**	**0.56**	**0.0043**	**0.0341**
Right superior corona radiata	0.89	0.38	1.97	0.7845	0.8335
Left superior corona radiata	1.23	0.53	2.84	0.6183	0.7007
Right posterior corona radiata	0.70	0.30	1.65	0.3982	0.4836
Left posterior corona radiata	0.66	0.28	1.56	0.3425	0.4314
Right posterior thalamic radiation	0.45	0.17	1.06	0.0772	0.1313
Left posterior thalamic radiation	0.33	0.10	0.85	0.0324	0.0782
Right superior longitudinal fasciculus	**0.31**	**0.11**	**0.73**	**0.0130**	**0.0471**
Left superior longitudinal fasciculus	0.40	0.17	0.87	0.0230	0.0653
Right inferior fronto-occipital fasciculus	0.60	0.21	1.51	0.3027	0.3959
Left inferior fronto-occipital fasciculus	0.51	0.16	1.36	0.2118	0.3001
Right uncinate fasciculus	0.48	0.19	1.13	0.0966	0.1564
Left uncinate fasciculus	0.74	0.31	1.74	0.4917	0.5765
Right tapetum	0.46	0.18	1.04	0.0670	0.1199
Left tapetum	0.39	0.15	0.91	0.0345	0.0782

Table 2. The associations between tract-specific FA and longitudinal SDMT scores decline. Logistic regression models were used to assess the associations between tract-specific FA values and longitudinal decline in SDMT scores at follow-up. Statistical significance was defined as a FDR-adjusted $P < 0.05$, with significant values presented in bold. Abbreviations: CI, confidence interval; OR, odds ratio; FDR, false discovery rate; SDMT, Symbol Digit Modalities Test.

The microstructural integrity of CC as a promising indicator of cognitive resilience

As shown in Tables 2 and 3 and Table S8, higher microstructural integrity in the genu, body, and splenium of the CC was associated with a reduced likelihood of decline in LNS and SDMT scores. To further illustrate these associations, we stratified PD patients into tertiles based on FA values in these CC subregions and conducted linear mixed-effects analysis for modelling time × white matter interactions at two time points. As illustrated in Fig. S1, PD patients in the higher FA tertile of the CC genu maintained stable cognitive profiles throughout the follow-up period. In contrast, those in the lower tertile exhibited significant declines in the scores of LNS and SDMT (FDR-corrected $P < 0.05$; Fig. S1A-B). Similarly, patients in the higher FA tertile of the CC body demonstrated relatively stable cognitive performance, while those in the lower tertile showed notably lower scores in LNS and SDMT compared to their higher tertile counterparts (FDR-corrected $P < 0.05$; Fig. S1C-D). For the splenium, patients in the lower FA tertile also showed significant declines in the scores of LNS and SDMT over time (FDR-corrected $P < 0.05$; Fig. S1E-F). Collectively, these results indicate that preserved microstructural integrity across CC subregions is associated with maintained cognitive performance in PD, reinforcing the view that intact white matter integrity may serve as a neuroprotective mechanism against cognitive decline.

Discussion

Our study comprehensively explored the relationships between white matter integrity and the progression of cognitive and motor symptoms in PD, providing preliminary evidence for the potential of white matter-based

Tracts Statistics	OR	Lower_CI	Upper_CI	*P*-value	FDR-corrected *P*-value
Genu of corpus callosum	**3.08**	**1.34**	**7.70**	**0.0089**	**0.0498**
Body of corpus callosum	**5.88**	**2.06**	**23.44**	**0.0029**	**0.0482**
Splenium of corpus callosum	**5.20**	**2.04**	**18.23**	**0.0022**	**0.0482**
Fornix	3.20	1.20	10.94	0.0347	0.0563
Right corticospinal tract	2.21	0.97	5.47	0.0659	0.0861
Left corticospinal tract	2.53	1.15	6.25	0.0262	0.0546
Right inferior cerebellar peduncle	2.19	0.94	5.93	0.0834	0.1012
Left inferior cerebellar peduncle	2.37	1.00	6.06	0.0524	0.0742
Right superior cerebellar peduncle	1.17	0.51	2.59	0.7022	0.7119
Left superior cerebellar peduncle	0.86	0.37	1.91	0.7119	0.7119
Right cerebral peduncle	**3.88**	**1.46**	**14.23**	**0.0167**	**0.0498**
Left cerebral peduncle	**5.33**	**1.69**	**27.59**	**0.0190**	**0.0498**
Right anterior limb of internal capsule	**2.63**	**1.22**	**6.45**	**0.0172**	**0.0498**
Left anterior limb of internal capsule	**2.73**	**1.23**	**6.90**	**0.0185**	**0.0498**
Right posterior limb of internal capsule	**3.99**	**1.39**	**14.87**	**0.0189**	**0.0498**
Left posterior limb of internal capsule	3.47	1.22	12.80	0.0324	0.0552
Right retrolenticular part of internal capsule	2.25	0.97	6.20	0.0766	0.0964
Left retrolenticular part of internal capsule	**2.90**	**1.30**	**7.69**	**0.0156**	**0.0498**
Right anterior corona radiata	2.45	1.10	5.81	0.0292	0.0546
Left anterior corona radiata	2.48	1.15	5.72	0.0219	0.0531
Right superior corona radiata	2.94	1.22	8.84	0.0286	0.0546
Left superior corona radiata	**4.42**	**1.63**	**15.13**	**0.0079**	**0.0498**
Right posterior corona radiata	1.86	0.84	4.35	0.1297	0.1521
Left posterior corona radiata	2.94	1.19	8.72	0.0305	0.0546
Right posterior thalamic radiation	1.31	0.59	2.90	0.4971	0.5282
Left posterior thalamic radiation	2.42	1.01	6.50	0.0548	0.0745
Right superior longitudinal fasciculus	2.38	1.06	5.94	0.0449	0.0663
Left superior longitudinal fasciculus	2.29	1.06	5.36	0.0396	0.0612
Right inferior fronto-occipital fasciculus	1.93	0.76	5.55	0.1856	0.2104
Left inferior fronto-occipital fasciculus	1.86	0.71	5.44	0.2201	0.2414
Right uncinate fasciculus	**3.99**	**1.76**	**13.24**	**0.0044**	**0.0482**
Left uncinate fasciculus	**2.64**	**1.23**	**6.24**	**0.0149**	**0.0498**
Right tapetum	2.73	1.19	7.40	0.0260	0.0546
Left tapetum	**3.61**	**1.52**	**10.01**	**0.0057**	**0.0482**

Table 3. The associations between tract-specific MD and longitudinal SDMT scores decline. Logistic regression models were used to assess the associations between tract-specific MD values and longitudinal decline in SDMT scores at follow-up. Statistical significance was defined as a FDR-adjusted $P < 0.05$, with significant values presented in bold. Abbreviations: CI, confidence interval; OR, odds ratio; FDR, false discovery rate; SDMT, Symbol Digit Modalities Test.

imaging metrics as prognostic biomarkers. In a previous cross-sectional study, we reported that white matter-based imaging metrics are associated with age-dependent cognitive impairment in patients with PD[8]. However, whether these white matter-based metrics are also associated with longitudinal cognitive and motor decline remained largely elusive. In the present study, we demonstrated that microstructural integrity within specific tracts, particularly subregions of the CC and the right ICP, may be a critical substrate of cognitive reserve, whose disruption is associated with future cognitive deterioration. These findings not only reinforce the role of white matter in cognitive preservation but also highlight its potential as an imaging biomarker for prognostic stratification in PD. Ultimately, this work supports the incorporation of white matter metrics into future predictive models to enhance early intervention and individualized management strategies for patients with PD.

The CC is located at the midline of the brain, situated above the lateral ventricles. It is a vital brain structure that facilitates communication between the cerebral hemispheres, playing essential roles in motor coordination, cognitive processing, and integration of sensory information[18]. A previous study showed that the volumes of the five segments of CC were comparable between PD and controls, indicating preserved gray matter integrity of CC in PD patients[19]. However, PD patients exhibit disrupted white matter integrity in the CC compared to healthy individuals[20,21]. The impairment of CC integrity is significantly associated with cognitive decline in PD patients, underscoring its relevance in the pathophysiology of cognitive impairment in this disease[20,22]. Additionally, another cross-sectional study showed that FA of CC correlates with semantic dysfunction in PD patients, further supporting the close relationship between microstructural changes of CC and cognitive capacity[23]. However, the

cross-sectional design of these studies limits the ability to establish causal relationships between CC integrity and cognitive deterioration in PD. Here, our longitudinal findings demonstrate that the microstructural integrity of specific CC subregions may be a critical indicator of cognitive resilience, with early microstructural disruption associated with subsequent cognitive decline. These findings align with emerging evidence on the critical role of CC in cognitive decline in PD, including Bledsoe et al..'s report linking CC integrity to cognitive impairment (2017 MDS International Congress, Abstract 1499)[20], and Brown et al..'s demonstration of association between free water in CC and cognitive impairment (MDS Virtual Congress 2020, Abstract 563) in PD patients. Our findings not only reinforce the importance of the CC in modulating cognitive function but also highlight its potential utility as a biomarker for early prediction. To advance beyond structural correlations, future studies may integrate functional neuroimaging to elucidate how CC subregions dynamically coordinate cognition[24]. Resting-state and task-based functional MRI could map connectivity patterns between CC-linked homologous cortices (e.g., prefrontal genu connections), testing whether disrupted interhemispheric synchrony mediates cognitive decline[24]. Complementarily, causal interrogation via transcranial magnetic stimulation applied to CC termination zones may transiently modulate callosal transfer efficiency[25,26], while intraoperative deep brain stimulation recordings could capture white matter signal propagation during cognitive tasks. These insights will accelerate drug development, high-throughput screening of myelination-enhancing compounds (e.g., Clemastine) in CC injury models offers actionable pathways toward cognition-preserving therapies.

The ICP is a crucial structure in the brain that serves as a major pathway connecting the cerebellum to the brainstem and the spinal cord. It plays a significant role in the integration of sensory and motor information, and recent research has begun to explore its implications for cognitive function, particularly in the context of neuropsychiatric diseases and other conditions affecting cognition. Our prior cross-sectional study revealed that FA of the bilateral ICP mediates the negative association between aging and cognitive decline in PD patients[8]. Current longitudinal data further suggest that a decline in FA within the right ICP may be associated with future cognitive deterioration, reinforcing the significant association between ICP integrity and cognitive decline in this population. Importantly, higher FA in the right ICP was associated with social impairment, highlighting its involvement in social cognition[27]. Similarly, a study found that FA in the left ICP correlates with social cognition deficits in individuals with Multiple sclerosis[28], suggesting a foundational role of ICP microstructural integrity in broader cognitive functions. Despite these significant insights, the precise role of the ICP in the regulation of cognitive impairment remains inadequately understood, warranting further investigation. Future research should aim to clarify the neuroanatomical or functional connections of the ICP with regions involved in cognitive processing, such as the prefrontal cortex and limbic structures, to elucidate the pathways through which the ICP influences cognitive functions. In summary, our findings underscore the importance of the ICP in understanding cognitive decline in PD. As research progresses, elucidating the mechanisms underlying ICP integrity and cognitive function will be crucial for developing targeted interventions aimed at preserving cognitive health in affected populations.

The assessment of white matter networks through graphical metrics such as GE, LE, and small-worldness Lp offers profound insights into the structural integrity of neural networks. In a previous study, we found lower global and local efficiency, as well as higher small-worldness Lp mediate the negative association between aging and cognitive decline in PD[8], indicating disrupted white matter network topology contributes to cognitive impairment. Building on this foundation, the present study extends these observations by identifying suggestive associations between topological properties and longitudinal cognitive decline, as indicated in Table S12. Although these relationships did not survive strict multiple comparison correction, their consistent directional trends reinforce the plausibility of white matter network disruption as a substrate of cognitive deterioration. Importantly, the convergence between prior and current findings highlights the potential utility of graph-based network measures as potential markers of neural change, even in the absence of full statistical significance in this cohort. This recurring pattern underscores the necessity of further investigating white matter topology in larger, longitudinal samples to clarify its role in cognitive progression and to evaluate its eventual utility as a prognostic indicator or therapeutic target in PD.

Our findings suggest that the microstructural integrity of specific white matter tracts, particularly the right superior longitudinal fasciculus, may be associated with motor decline in PD, although these associations did not survive FDR correction (Tables S13–S14). As the largest associative fiber bundle in the brain, the superior longitudinal fasciculus forms critical connections between the frontal lobe and other ipsilateral regions[29,30]. Functionally, its dorsal component is implicated in visuospatial attention and motor control, while the ventral stream supports language and auditory processing, particularly in the left hemisphere[29,30]. Prior study has demonstrated reduced integrity in the superior longitudinal fasciculus of PD patients[31], and recent evidence links its impairment to motor progression in *GBA1*-mutation carriers[32]. Nevertheless, the precise mechanistic pathways through which the microstructure integrity of superior longitudinal fasciculus influences motor symptoms remain unclear. Future studies should combine advanced multimodal imaging, assessing both structural and functional connectivity, to clarify how the microstructure of superior longitudinal fasciculus contributes to specific motor manifestations in PD. Elucidating these mechanisms will not only deepen our understanding of PD pathophysiology but may also guide the development of targeted therapies to slow motor symptom progression.

The current research has several limitations that should be addressed in future studies. One significant limitation is the relatively short follow-up period of 3–5 years, which may not capture the long-term trajectory of cognitive and motor decline in patients with PD. This limited timeframe restricts our understanding of the temporal dynamics between white matter integrity and the progression of symptoms. Additionally, the reliance on a relatively small sample size may hinder the generalizability of the findings across diverse PD populations. Furthermore, further research is necessary to explore the underlying neurobiological mechanisms that link white matter changes to cognitive outcomes. Finally, it is important to acknowledge the methodological limitations

associated with the deterministic tractography approach employed in this study. The use of the Fiber Assignment by Continuous Tracking (FACT) algorithm, coupled with the applied thresholds (FA > 0.20, angle < 45°), inherently constrains the accurate reconstruction of white matter pathways in regions with complex fiber architectures, such as crossing, kissing, or fanning fibers. This limitation primarily arises from the inability of the tensor model to resolve multiple fiber orientations within a single voxel, leading to partial volume effects that can compromise the anatomical accuracy of streamline trajectories at intricate white matter junctions. Looking forward, the application of advanced reconstruction techniques, such as constrained spherical deconvolution, which directly models multiple fiber populations, holds significant promise for elucidating the finer details of white matter organization in PD. By providing a more biologically plausible representation of underlying fiber geometry, such methods could substantially refine our understanding of structure-function relationships and offer deeper insights into the network-level pathophysiology associated with cognitive and motor decline. This study, therefore, while providing a robust initial mapping based on conventional methodology, also establishes a clear rationale and foundation for subsequent investigations utilizing these more advanced, high-fidelity tractography frameworks. Together, addressing above limitations through longer-term, larger-scale, longitudinal studies integrating advanced tractography and multimodal techniques will be crucial for validating white matter-based imaging metrics as reliable predictive biomarkers in PD, ultimately enhancing our ability to develop effective therapeutic strategies.

In conclusion, our study provides preliminary evidence that preserved microstructural integrity within key cerebral white matter tracts, most notably the CC, may be a robust and biologically relevant indicator of cognitive resilience in PD. Importantly, the quantitative nature of these imaging metrics opens the possibility of identifying at-risk patients during early or even presymptomatic stages, well before significant cognitive deficits become clinically apparent. Such early detection could critically inform the timing and selection of personalized interventions, whether pharmacological, cognitive, or lifestyle-based, aimed at delaying or mitigating the progression of cognitive impairment. Ultimately, integrating white matter integrity assessments into standard prognostic evaluation may help transition PD cognitive care toward a more preventive and patient-tailored paradigm, with meaningful implications for long-term neurological outcomes and quality of life.

Methods and materials

Ethics

Data utilized in this investigation were obtained from the PPMI database (http://www.ppmi-info.org), which is publicly accessible. The PPMI study procedures received approval from the Institutional Review Boards of all participating centers, and informed consent was obtained from all participants prior to their participation of the study. All data were anonymized to ensure participant confidentiality. The utilization of this data was approved by the PPMI, and all methods were performed in accordance with relevant guidelines and regulations to ensure ethical compliance.

Participants

PPMI is an international multicenter cohort study enrolling over 400 patients diagnosed with early-stage PD and 200 healthy individuals who acted as controls[33,34]. All participants underwent a range of standardized assessments, including imaging, biochemical tests, clinical evaluations, and behavioral assessments, aimed at facilitating the exploration of predictive biomarkers for PD progression. For the latest information regarding PPMI study, please visit http://www.ppmi-info.org. The inclusion criteria for PD patients included: (i) being over 30 years old; (ii) having a diagnosis of PD based on the clinical diagnostic criteria from the International Parkinson and Movement Disorder Society; (iii) having completed both 3D T1-weighted imaging and DTI within the same timeframe; and (iv) undergoing assessments of motor and cognitive symptoms over a follow-up period of 3 to 5 years. Participants were excluded if they showed significant abnormalities in T1-weighted or T2-weighted MRI scans, had genetic mutations associated with familial PD, or were part of either the genetic PPMI cohort or the prodromal cohort. Following these inclusion and exclusion criteria, a total of 121 PD patients were included in the analysis. Motor evaluations primarily utilized UPDRS-III, while cognitive assessments included SFT, LNS, MoCA, and SDMT. The clinical characteristics of PD patients at baseline and follow-up are detailed in Table 1; Fig. 1. Baseline data from 121 age- and sex-matched healthy control participants receiving MRI scans enrolled in the PPMI cohort were additionally included and analyzed (Table 1). There were no significant differences in age ($P > 0.05$) or years of education ($P > 0.05$) between the PD and healthy control group at baseline (Table 1). As this study specifically focuses on identifying white matter-based metrics for predicting longitudinal cognitive and motor outcomes in PD, the healthy control cohort was used solely to establish a reference for defining baseline cognitive impairment in the PD group, as is common in normative comparison approaches.

Image acquisition

The structural and functional imaging data were obtained using Siemens 3T Trio or Verio scanners, manufactured by Siemens Medical Solutions in Malvern, PA. The 3D T1-weighted MRI images were produced with a magnetization-prepared rapid acquisition gradient echo sequence, which had the following parameters: Repetition time (TR) of 2300 ms, Echo time (TE) of 2.98 ms, Voxel size of 1 mm^3, Slice thickness of 1.2 mm, twofold acceleration, and sagittal-oblique angulation. For DTI, the parameters used were: TR of 8,400-8,800 ms, TE of 88 ms, Voxel size of 2 mm^3, Slice thickness of 2 mm, 64 diffusion-sensitive gradient directions at $b = 1{,}000$ s/mm^2, and one diffusion-unweighted (b0) image.

Imaging preprocessing

The preprocessing of DTI images for 121 PD patients was performed using the FMRIB Software Library toolkit (FSL, available at https://fsl.fmrib.ox.ac.uk/fsl/fslwiki). A rigorous quality control (QC) protocol was

implemented both before and during processing to ensure data integrity. Prior to analysis, all raw DTI volumes underwent visual inspection for artifacts, including signal dropout, ghosting, and excessive motion. Initial DTI preprocessing leveraged integrated correction pipeline in FSL, commencing with comprehensive artifact mitigation: Rigid-body motion correction was performed using *mcflirt* with normalized mutual information cost function and 6° of freedom, compensating for head displacement between volumes. Subsequent eddy processing addressed both eddy current distortions and susceptibility-induced echo-planar imaging deformations through simultaneous quadratic phase modeling and slice-to-volume correction with b-vector rotation enabled. Crucially, the *eddy_cuda* implementation incorporated outlier slice detection via Gaussian process modeling, automatically replacing contaminated slices where signal deviation exceeded 4 SD from predicted values. Gradient nonlinearity correction was applied using manufacturer-specific coefficients, while physiological noise was suppressed via topup-based field map estimation. This multi-stage protocol followed FSL's best practices for neurodegenerative cohorts, significantly reducing motion-related bias in diffusivity metrics critical for PD analysis. Following preprocessing, a second QC step was conducted, including visual assessment of tractography reconstruction quality and quantitative evaluation of alignment accuracy in standard MNI space. No individual datasets were excluded from the initial dataset pool due to issues including excessive motion artifacts or failed processing. Subsequently, metrics such as FA and MD were calculated for 34 white matter tracts (shown in Tables 2 and 3) from Johns Hopkins University ICBM-DTI atlas. The preprocessing steps for the DTI images have been described in detail in our previous studies[9].

Network construction

Structural networks were created using deterministic fiber tractography through the free MATLAB toolkit called PANDA (http://www.nitrc.org/projects/panda/). Network nodes were defined according to the 90-region Automated Anatomical Labeling (AAL) atlas encompassing cortical and subcortical structures. Deterministic whole-brain tractography was implemented via the Fiber Assignment by Continuous Tracking (FACT) algorithm with conservative tracking constraints: FA threshold = 0.20 to minimize spurious connections in gray matter, and maximum fiber turning angle = 45° to respect neuroanatomical curvature limits. For each participant, inter-nodal connectivity was quantified by enumerating streamlines terminating between region pairs, generating individual 90 × 90 structural connectivity matrices. Since the structural network matrices created using FA and streamline counts displayed similar network topology[9,35], consequently, we exclusively analyzed streamline count-based matrices to prioritize biological interpretability of structural connectivity strength while maintaining computational efficiency and consistency with established structural network methodologies in neurodegenerative research.

Graph-based network analysis

The GRETNA toolbox (https://www.nitrc.org/projects/gretna/) was utilized to analyze the topological properties of the structural network. To ensure robustness against arbitrary threshold selection, we implemented a multi-threshold strategy across a sparsity range of 0.05 to 0.50 (increments = 0.05), systematically controlling edge density while preserving relative network organization. At each of the 10 sparsity levels, global topological metrics were computed, including GE, LE, and small-worldness metrics (Cp, Lp, γ, λ, and σ). Crucially, the AUC for each metric was calculated by integrating values across all thresholds, providing a summarized measure insensitive to single-threshold selection bias and enhancing biological interpretability. This AUC approach effectively captures the topological trajectory across network densities, reflecting organizational principles resilient to connection density variations. All metric definitions adhered to established neuroimaging standards: Cp measured functional segregation efficiency, Lp characterized integration capacity, while $\gamma > 1$ and $\lambda \approx 1$ confirmed small-world topology. Computational procedures followed precisely defined formulae documented in prior methodological references[36,37], ensuring reproducibility of each metric computation.

Statistical analysis

Statistical analyses were conducted using GraphPad Prism (Version 8.0.2) and R Statistical Environment (Version 4.5.0). Before hypothesis testing, the distributional properties of all continuous variables, including clinical assessment scores and white matter-based metrics, were rigorously evaluated. Normality was assessed using two complementary omnibus tests: the Shapiro-Wilk test and the Anderson-Darling test. Variables violating normality assumptions ($\alpha = 0.05$) were subsequently analyzed using nonparametric methodologies. Baseline comparisons of clinical variables between control and PD groups were conducted using unpaired Student's t-tests or χ^2 tests, as appropriate. Longitudinal clinical changes between baseline and follow-up were assessed via two-tailed paired Student's t-tests for Gaussian-distributed variables, supplemented by Wilcoxon signed-rank tests for non-normal distributions.

The normative data employed in this study were primarily derived from healthy control and PD participants assessed at their baseline visit within the PPMI cohort. Clinically meaningful cognitive decline was defined using a consistent threshold of >2 SD below reference means, applied separately for cross-sectional and longitudinal assessments. At baseline, patients were classified as having cognitive impairment if their score fell more than 2 SD below the healthy control mean on one or more neuropsychological tests. For longitudinal evaluation, decline was correspondingly defined as a decrease of more than 2 SD below the baseline mean of the PD cohort on one or more tests during follow-up. Binary logistic regression models evaluated the associations between white matter metrics and cognitive impairment at both cross-sectional (baseline) and longitudinal (follow-up) stages, with hierarchically adjusted covariates: baseline models incorporated age, sex, education years, and disease duration; longitudinal models additionally included follow-up duration and baseline cognition. The associations between white matter metrics and changes in UPDRS-III and total UPDRS scores at both cross-sectional and longitudinal stages were assessed using the similar statistical approaches as shown above. Model robustness was

verified through Hosmer-Lemeshow goodness-of-fit tests and variance inflation factors (VIF < 2.5 confirming multicollinearity absence). OR and 95% CI for each tract-cognitive score relationship were reported for each cognitive assessment (MoCA, LNS, SDMT). Separate FDR corrections were applied for all 34 tract-level analyses for each cognitive scale to control type I error, with FDR-corrected $P < 0.05$ defining statistical significance.

To better show the significant effects of white matter integrity on cognitive decline, the PD participants ($n = 121$) were categorized into three tertile groups based on imaging metric values: lower tertile group (metric value rank: 0%–33.33%), middle tertile group (metric value rank: 33.33%–66.66%), and higher tertile group (metric value rank: 66.66%–100%). Group differences in cognitive assessments across different tertile groups were assessed using linear mixed-effects models, followed by FDR corrections for multiple comparisons. This tract-specific tertile approach is strictly limited to the genu, body, and splenium of CC, which exhibited significant associations with longitudinal cognitive decline in SDMT scores (Tables 2 and 3). FDR-corrected $P < 0.05$ was considered statistically significant.

Data availability

The data may be available upon reasonable request to the corresponding author.

Received: 5 March 2025; Accepted: 25 November 2025
Published online: 05 December 2025

References

1. Bloem, B. R., Okun, M. S. & Klein, C. Parkinson's disease. *Lancet* **397**, 2284–2303 (2021).
2. Collaborators, G. B. D. N. Global, regional, and National burden of neurological disorders, 1990–2016: a systematic analysis for the global burden of disease study 2016. *Lancet Neurol.* **18**, 459–480 (2019).
3. Aarsland, D. et al. Parkinson disease-associated cognitive impairment. *Nat. Rev. Dis. Primers.* **7**, 47 (2021).
4. Pan, C. et al. Characterizing mild cognitive impairment in prodromal parkinson's disease: A community-based study in China. *CNS Neurosci. Ther.* **28**, 259–268 (2022).
5. Guner, D., Tiftikcioglu, B. I., Tuncay, N. & Zorlu, Y. Contribution of quantitative EEG to the diagnosis of early cognitive impairment in patients with idiopathic parkinson's disease. *Clin. EEG Neurosci.* **48**, 348–354 (2017).
6. Gan, Y. et al. Association between Cognitive Impairment and Freezing of Gait in Patients with Parkinson's Disease. *J Clin. Med* **12**, 2799 (2023).
7. Owens-Walton, C. et al. A worldwide study of white matter microstructural alterations in people living with parkinson's disease. *NPJ Parkinsons Dis.* **10**, 151 (2024).
8. Chen, Z. et al. Age and sex differentially shape brain networks in parkinson's disease. *CNS Neurosci. Ther.* **29**, 1907–1922 (2023).
9. Chen, Z. et al. MAPT rs17649553 T allele is associated with better verbal memory and higher small-world properties in parkinson's disease. *Neurobiol. Aging.* **129**, 219–231 (2023).
10. Theilmann, R. J. et al. White-matter changes correlate with cognitive functioning in parkinson's disease. *Front. Neurol.* **4**, 37 (2013).
11. de Oliveira, P., Martins, B. J. & Cardoso, F. E. C. White matter hyperintensity presence, quantity, and location exhibits no association with motor and non-motor manifestations of PD. *Parkinsonism Relat. Disord.* **106**, 105245 (2023).
12. de Carvalho, D. C. et al. White matter hyperintensity burden predicts cognitive but not motor decline in parkinson's disease: results from the Ontario neurodegenerative diseases research initiative. *Eur. J. Neurol.* **30**, 920–933 (2023).
13. Wu, H. et al. Regional white matter hyperintensity volume in parkinson's disease and associations with the motor signs. *Ann. Clin. Transl Neurol.* **10**, 1502–1512 (2023).
14. Carvalho de Abreu, D. C., Pieruccini-Faria, F., Son, S., Montero-Odasso, M. & Camicioli, R. Is white matter hyperintensity burden associated with cognitive and motor impairment in patients with parkinson's disease? A systematic review and meta-analysis. *Neurosci. Biobehav Rev.* **161**, 105677 (2024).
15. Yang, K. et al. White matter changes in parkinson's disease. *NPJ Parkinsons Dis.* **9**, 150 (2023).
16. Jiang, Y. Q. et al. White matter lesions contribute to motor and non-motor disorders in parkinson's disease: a critical review. *Geroscience* **47**, 591–609 (2025).
17. Zhao, B. et al. Common genetic variation influencing human white matter microstructure. *Science* **372**, eabf3736 (2021).
18. Ribeiro, M., Yordanova, Y. N., Noblet, V., Herbet, G. & Ricard, D. White matter tracts and executive functions: a review of causal and correlation evidence. *Brain* **147**, 352–371 (2024).
19. Lenka, A. et al. Role of corpus callosum volumetry in differentiating the subtypes of progressive supranuclear palsy and early parkinson's disease. *Mov. Disord Clin. Pract.* **4**, 552–558 (2017).
20. Bledsoe, I. O., Stebbins, G. T., Merkitch, D. & Goldman, J. G. White matter abnormalities in the corpus callosum with cognitive impairment in Parkinson disease. *Neurology* **91**, e2244–e2255 (2018).
21. Pietracupa, S. et al. White and Gray matter alterations in de Novo PD patients: which matter most? *J. Neurol.* **270**, 2734–2742 (2023).
22. Kamagata, K. et al. Relationship between cognitive impairment and white-matter alteration in parkinson's disease with dementia: tract-based Spatial statistics and tract-specific analysis. *Eur. Radiol.* **23**, 1946–1955 (2013).
23. Liu, H. et al. Corpus callosum and cerebellum participate in semantic dysfunction of parkinson's disease: a diffusion tensor imaging-based cross-sectional study. *Neuroreport* **35**, 366–373 (2024).
24. Wang, P. et al. Structural and functional connectivity mapping of the human corpus callosum organization with white-matter functional networks. *Neuroimage* **227**, 117642 (2021).
25. Voineskos, A. N. et al. The role of the corpus callosum in transcranial magnetic stimulation induced interhemispheric signal propagation. *Biol. Psychiatry.* **68**, 825–831 (2010).
26. Chechlacz, M., Humphreys, G. W., Sotiropoulos, S. N., Kennard, C. & Cazzoli, D. Structural organization of the corpus callosum predicts attentional shifts after continuous theta burst stimulation. *J. Neurosci.* **35**, 15353–15368 (2015).
27. Ramphal, B., Pagliaccio, D., Thomas, L. V., He, X. & Margolis, A. E. Contributions of cerebellar white matter microstructure to social difficulty in nonverbal learning disability. *Cerebellum* **20**, 931–937 (2021).
28. Batista, S. et al. Disconnection as a mechanism for social cognition impairment in multiple sclerosis. *Neurology* **89**, 38–45 (2017).
29. Nakajima, R., Kinoshita, M., Shinohara, H. & Nakada, M. The superior longitudinal fascicle: reconsidering the fronto-parietal neural network based on anatomy and function. *Brain Imaging Behav.* **14**, 2817–2830 (2020).
30. Janelle, F., Iorio-Morin, C., D'Amour, S. & Fortin, D. Superior longitudinal fasciculus: A review of the anatomical descriptions with functional correlates. *Front. Neurol.* **13**, 794618 (2022).
31. Wei, X. et al. Gait impairment-related axonal degeneration in parkinson's disease by neurite orientation dispersion and density imaging. *NPJ Parkinsons Dis.* **10**, 45 (2024).

32. Yu, C. H., Rodriguez-Porcel, F., Wilson, S., Lench, D. H. & Cooper, C. A. Genetic influence on microstructure integrity and motor progression in parkinson's disease. *Parkinsonism Relat. Disord.* **127**, 107082 (2024).
33. Parkinson Progression Marker Initiative. The Parkinson progression marker initiative (PPMI). *Prog Neurobiol.* **95**, 629–635 (2011).
34. Marek, K. et al. The parkinson's progression markers initiative (PPMI) - establishing a PD biomarker cohort. *Ann. Clin. Transl Neurol.* **5**, 1460–1477 (2018).
35. Zhao, L. et al. Brain white matter structural networks in patients with non-neuropsychiatric systemic lupus erythematosus. *Brain Imaging Behav.* **12**, 142–155 (2018).
36. Rubinov, M. & Sporns, O. Complex network measures of brain connectivity: uses and interpretations. *Neuroimage* **52**, 1059–1069 (2010).
37. Wang, J. H. et al. Graph theoretical analysis of functional brain networks: test-retest evaluation on short- and long-term resting-state functional MRI data. *PLoS One.* **6**, e21976 (2011).

Acknowledgements

This study was supported by grants from the National Natural Science Foundation of China (82230040, 82341251, and 82360230), the Hainan Provincial Natural Science Foundation of China (825MS173), the Scientific Research Project of Hainan Higher Education Institutions (Hnky2025-21), the Academic Advancement Program of Hainan Medical University (XSTS2025116), the Shanghai Research Doctor Program (SHDC2023CRT014), the Shanghai Heath Commission Research Program (202440091) and the Shanghai Jiaotong University STAR Program (20220103).

Author contributions

Zhichun Chen: Writing – original draft, Formal analysis, Methodology. Weiting Tang: Writing – review & editing, Formal analysis. Yuxuan Shi: Formal analysis. Jindong Ding Petersen: Writing – review & editing, Data curation. Binwen Huang: Software, Visualization, Jun Liu and Yong You: Writing – Supervision, Funding acquisition. All authors reviewed the manuscript.

Declarations

Competing interests

The authors declare no competing interests.

Additional information

Supplementary Information The online version contains supplementary material available at https://doi.org/10.1038/s41598-025-30478-4.

Correspondence and requests for materials should be addressed to J.L. or Y.Y.